Tangential migration of neuronal precursors of glutamatergic neurons in the adult mammalian brain

Gerald J. Sun[a,b,1], Yi Zhou[a,c,1], Ryan P. Stadel[a,d,1], Jonathan Moss[e], Jing Hui A. Yong[f], Shiori Ito[a], Nicholas K. Kawasaki[a], Alexander T. Phan[a], Justin H. Oh[a], Nikhil Modak[a], Randall R. Reed[b,g,h], Nicolas Toni[e], Hongjun Song[a,b,c,d,f,i,2], and Guo-li Ming[a,b,c,f,h,j,2]

[a]Institute for Cell Engineering, Johns Hopkins University School of Medicine, Baltimore, MD 21205; [b]The Solomon H. Snyder Department of Neuroscience, Johns Hopkins University School of Medicine, Baltimore, MD 21205; [c]Biochemistry, Cellular and Molecular Biology Graduate Program, Johns Hopkins University School of Medicine, Baltimore, MD 21205; [d]Predoctoral Human Genetics Training Program, Johns Hopkins University School of Medicine, Baltimore, MD 21205; [e]Department of Fundamental Neurosciences, University of Lausanne, 1005 Lausanne, Switzerland; [f]Cellular and Molecular Medicine Graduate Program, Johns Hopkins University School of Medicine, Baltimore, MD 21205; [g]Center for Sensory Biology, Johns Hopkins University School of Medicine, Baltimore, MD 21205; [h]Department of Molecular Biology and Genetics, Johns Hopkins University School of Medicine, Baltimore, MD 21205; [i]Department of Neurology, Johns Hopkins University School of Medicine, Baltimore, MD 21205; and [j]Department of Psychiatry and Behavioral Sciences, Johns Hopkins University School of Medicine, Baltimore, MD 21205

Edited by Fred H. Gage, Salk Institute for Biological Studies, San Diego, CA, and approved June 23, 2015 (received for review May 2, 2015)

In a classic model of mammalian brain formation, precursors of principal glutamatergic neurons migrate radially along radial glia fibers whereas GABAergic interneuron precursors migrate tangentially. These migration modes have significant implications for brain function. Here we used clonal lineage tracing of active radial glia-like neural stem cells in the adult mouse dentate gyrus and made the surprising discovery that proliferating neuronal precursors of glutamatergic granule neurons exhibit significant tangential migration along blood vessels, followed by limited radial migration. Genetic birthdating and morphological and molecular analyses pinpointed the neuroblast stage as the main developmental window when tangential migration occurs. We also developed a partial "whole-mount" dentate gyrus preparation and observed a dense plexus of capillaries, with which only neuroblasts, among the entire population of progenitors, are directly associated. Together, these results provide insight into neuronal migration in the adult mammalian nervous system.

adult neurogenesis | lineage tracing | migration | hippocampus | vascular niche

The nervous system is formed by migration of neuronal precursors and immature neurons to specific locations during development. The classic radial unit hypothesis of mammalian brain development postulates that in the developing neocortex, glutamatergic, excitatory, principal neurons migrate radially to form discrete information-processing columns of ontogenetic origin (1), whereas GABAergic, inhibitory, modulatory interneurons migrate tangentially across columns (2). Neurogenesis persists in the adult mammalian brain in two primary regions and is thought to follow the classic migration model (3, 4). In the subventricular zone (SVZ) of the lateral ventricles, new neurons generated from neural precursors migrate tangentially to the olfactory bulb to become GABAergic interneurons (5, 6). In contrast, in the subgranular zone (SGZ) of the dentate gyrus, new neurons generated from radial glia-like neural stem cells (RGLs) migrate radially into the granule cell layer to become principal glutamatergic granule cells (7). Due to technical challenges, migratory patterns have only been examined at the cell-population level, and thus we still lack detailed information about the spatial relationship between individual precursors and their progeny in vivo. Both adult neurogenic niches are highly vascularized, and this property is hypothesized to play a critical role in adult neurogenesis (3). In both adult SVZ (8–10) and SGZ (11), proliferating progenitor cells are in close association with the vasculature, yet the functional role of the vasculature in the niche remains to be fully explored.

Contrary to the classic model, our recent clonal lineage tracing of individual quiescent RGLs showed tangential distribution of glutamatergic granule neurons with respect to their parental RGL in the adult dentate gyrus (12). We therefore systematically investigated the migration pattern and trajectory of these newborn cells. Using a clonal lineage-tracing approach that preferentially targets active RGLs in the adult mouse dentate gyrus, thereby birthdating their newborn progeny in vivo, we found significant tangential distribution of newborn neuroblasts from their parental RGL. Furthermore, neuroblasts directly contact the vascular network, suggesting an important function of blood vessels as a substrate for migration. Together, our results reveal a previously unidentified mode of glutamatergic neuronal migration under physiological conditions in the adult mammalian brain.

Results

Spatial Distribution of Clonally Related Newborn Neuronal Progeny with a Defined Birthdate. We used a tamoxifen-inducible *Ascl1*^{CreERT2} knockin mouse line (13) to sparsely label (~8–16 cells per dentate gyrus) and lineage-trace clones of neural precursors in the adult dentate gyrus (Fig. 1*A*), following our previous strategy of clonally labeling RGLs using the *Nestin*^{CreERT2} mouse line (12). At 1 d post-tamoxifen injection (1 dpi), labeled cells in the adult SGZ consisted of over 90% Nestin^{+}GFAP^{+} RGLs and a few early intermediate progenitor cells (IPCs; $n = 8$ dentate gyri), as assessed by morphology

Significance

Mammalian brain development is a complex, ordered process whereby newborn neurons follow stereotyped migration modes to organize into specific patterns required for complicated neural circuit formation. Classically, principal excitatory neurons are thought to organize into radial columns that underlie the basic brain circuits, whereas inhibitory neurons disperse tangentially across these columns to modulate the principal circuits. These principles are thought to be fundamental to the genesis of the complex mammalian brain. Surprisingly, we found that precursors for excitatory principal neurons exhibit tangential migration in the adult mammalian brain. Our findings enrich our understanding of neurodevelopment and lay important conceptual groundwork for studies of brain plasticity, disease, and repair.

Author contributions: G.J.S., Y.Z., H.S., and G.-l.M. designed research; G.J.S., Y.Z., R.P.S., J.M., J.H.A.Y., S.I., N.K.K., A.T.P., J.H.O., N.M., and N.T. performed research; R.R.R. contributed new reagents/analytic tools; G.J.S., Y.Z., J.M., J.H.A.Y., S.I., N.K.K., A.T.P., J.H.O., N.M., and N.T. analyzed data; and G.J.S., Y.Z., H.S., and G.-l.M. wrote the paper.

The authors declare no conflict of interest.

This article is a PNAS Direct Submission.

[1]G.J.S., Y.Z., and R.P.S. contributed equally to this work.

[2]To whom correspondence may be addressed. Email: shongju1@jhmi.edu or gming1@jhmi.edu.

This article contains supporting information online at www.pnas.org/lookup/suppl/doi:10.1073/pnas.1508545112/-/DCSupplemental.

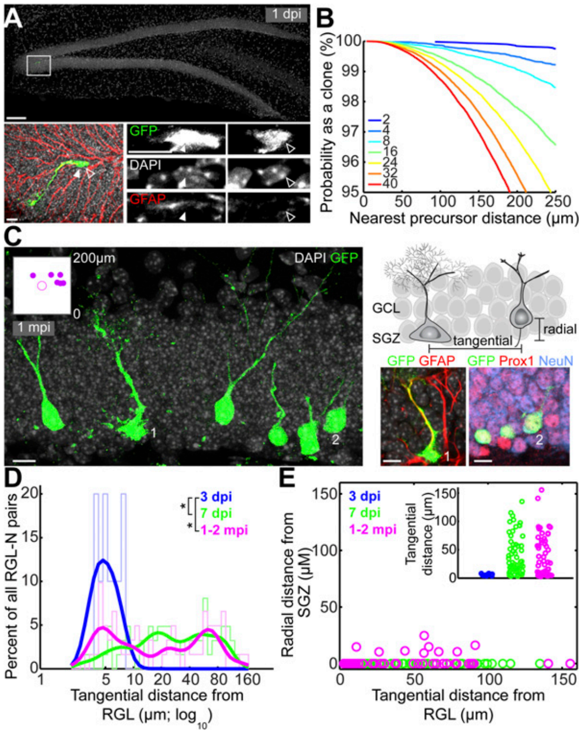

Fig. 1. Tangential distribution of newborn granule neurons away from their parental RGLs of origin in the adult dentate gyrus as revealed by in vivo clonal analysis. (*A*) Sample projected confocal image of an *Ascl1*^{CreERT2};*Rosa-YFP*$^{f/+}$–labeled RGL in the dentate gyrus at 1 dpi. As shown in a high-magnification image (*Bottom*), this GFAP$^+$ RGL (closed arrowheads) underwent an asymmetric division to produce a GFAP$^-$ neuronal progeny (open arrowheads; on a different focal plane). [Scale bars, 100 μm (*Top*) and 10 μm (*Bottom*).] (*B*) Computational simulations of the nearest distances between two cells in the 3D dentate gyrus space. Each colored line represents the reverse cumulative distribution of the nearest cell distances from a simulation with a given number of total cells. (*C*) (*Left*) Sample projection confocal image of a labeled clone in an *Ascl1*^{CreERT2};*Rosa-YFP*$^{f/+}$ mouse at 1 mpi (Movie S1) showing tangential distribution of Prox1$^+$NeuN$^+$ mature glutamatergic granule neurons and their parental GFAP$^+$ RGL. (*Inset*) Two-dimensional SGZ plane projection in 200-μm-square windows of all clonally related cell locations. The RGL is represented as the center open circle; neural progeny are represented as closed circles. (*Right*, *Top*) Schematic diagram for measurements of tangential and radial distances of neuronal progeny from the parental RGL. (*Right*, *Bottom*) Enlarged confocal images for a GFAP$^+$ RGL (1) and Prox1$^+$NeuN$^+$ mature neuronal progeny (2). (Scale bars, 10 μm.) GCL, granule cell layer. (*D*) Distribution plot of the tangential distance between a labeled RGL and its progeny within each clone at 3 dpi, 7 dpi, and 1–2 mpi (*$P < 0.05$; two-sample Kolmogorov–Smirnov test statistic: 0.85 for 3 vs. 7 dpi; 0.66 for 3 dpi vs. 1–2 mpi). Raw distributions are shown as bar graphs; curved lines correspond to smoothed distributions. (*E*) Dot plot of the tangential versus radial distance from the parental RGL for each neural progeny in all labeled RGL-containing clones at 3 dpi, 7 dpi, and 1–2 mpi. (*Inset*) Tangential distance of each neural progeny from its parental RGL.

and molecular marker expression (Table S1). Computational simulations (12) estimated that given eight initially labeled cells, any two labeled cells within 200 μm of each other had a 99% probability of belonging to the same clone (Fig. 1*B*). Thus, although few isolated IPCs were labeled at 1 dpi, the probability of their misassignment to an RGL clone was 1% or lower. Crucially, given our simulation results, we conservatively conducted all our analyses by excluding clones in which progeny were >150 μm away from their parent RGL, thus only focusing on clones with a maximum diameter of 300 μm.

In contrast to *Nestin*^{CreERT2}-based clonal lineage tracing of quiescent RGLs that exhibited stochastic activation over time (12), at 1 dpi the majority of *Ascl1*^{CreERT2}-labeled RGLs (96 ± 2%, n = 10 dentate gyri) had just divided (with one adjacent progeny) or were in the process of cell division (Fig. 1*A*). Therefore, our current approach selectively targets activating RGLs, allowing, to our knowledge for the first time, birthdating of RGL progeny to track their development with high temporal precision. At 1 month posttamoxifen injection (mpi), we observed clones in which Prox-1$^+$NeuN$^+$ mature dentate granule cells were distributed a long distance (more than 100 μm) away from their mother RGL along the SGZ plane (Fig. 1*C* and Movie S1). These results suggest, in contrast to the classic model, tangential migration of a glutamatergic neuronal subtype in the adult mammalian brain under physiological conditions.

Developmental Stage-Specific Tangential Distribution. Newborn cells may exhibit tangential distribution due to passive mechanisms such as displacement upon cell division. To provide further evidence for active tangential migration, we explored the dynamics of cell distribution by time-course analysis. At 3 dpi, labeled cells exhibited little displacement from each other, despite all being identified as highly proliferative IPCs (14) (Fig. 1*D*). In contrast, at 7 dpi there was significant distance along the tangential plane of the SGZ between labeled newborn neural progenitors and their parental RGLs, the distribution of which was very similar to that at 1–2 mpi (Fig. 1*D*). Only ∼15% of labeled new neurons exhibited measurable radial displacement away from the SGZ into the granule cell layer even at 1 or 2 mpi (all <25 μm), yet among these cells ∼47% spread more than 25 μm tangentially away from their parental RGL (Fig. 1*E*). The average tangential distance exceeded that of radial distance by almost 18-fold. Notably, radial migration was absent at 7 dpi, suggesting that tangential movement preceded any radial migration (Fig. 1*E*); no correlation between tangential and radial migration was observed among individual cells that exhibited both (Fig. 1*E*; $R = 0.08$, $P = 0.85$). Taken together, these results establish that tangential distribution of newborn progeny from their parental RGL could not have arisen by chance and instead represents the dominant mode of migration in the adult dentate gyrus.

We next asked whether tangential migration occurred during a specific developmental stage (or stages) during adult neurogenesis. Adult hippocampal neurogenesis proceeds in a stereotypic sequence—dividing RGLs give rise to IPCs, which in turn develop through neuroblast and immature neuron stages before becoming mature glutamatergic granule neurons (Fig. 2*A*) (4). Using morphological features and molecular markers to distinguish labeled cells at different developmental stages (Fig. 2*A* and Table S1), we found that neuroblasts, corresponding to 3- to 7-d-old DCX$^+$ cells with a bipolar, elongated morphology, were the earliest cells in the developmental lineage that showed tangential distribution away from their parental RGL (Fig. 2*B*). On average, neuroblasts, immature neurons, and mature neurons exhibited similar tangential distances away from their parental RGLs (Fig. 2*B*). These results suggest that the majority of tangential migration occurs within the neuroblast stage during adult hippocampal neurogenesis.

Pattern and Magnitude of Tangential Distribution. A consequence of tangential migration of neuronal progeny is that individual clones disperse over areas beyond that of a radial unit, potentially allowing individual RGLs to modify a large domain of the hippocampal circuitry via neurogenesis. We visualized 2D SGZ projections of clones over time in 300-μm-square windows (Fig. S1; excluding clones with single RGLs that had not completed division). We also included non–RGL-containing clones only for 1–2 mpi, because in some clones RGLs became differentiated (12). Qualitatively, clones dispersed over large areas, strongly suggestive of widespread tangential migration (Fig. S1).

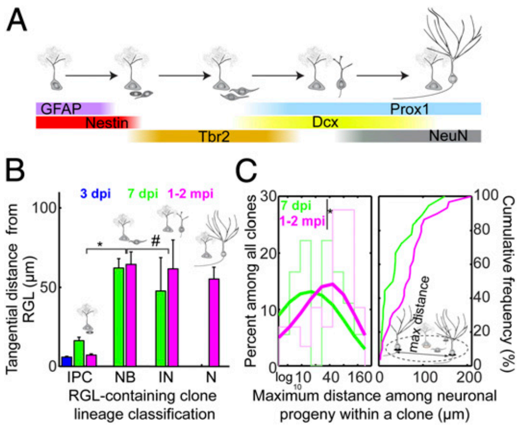

Fig. 2. Developmental stage-specific tangential distribution of newborn neural progeny. (*A*) Summary of molecular markers used for identification of each cell type during adult hippocampal neurogenesis. Newborn cells are generated from GFAP$^+$Nestin$^+$ RGLs that undergo asymmetric neuronal divisions, which develop into Tbr2$^+$ intermediate progenitor cells with short, multipolar processes within 3 d of birth. Within 3–7 d, newborn cells possess long, bipolar processes and elongated somas in a Tbr2$^{+/-}$DCX$^+$ neuroblast stage before penetrating the granule cell layer and becoming a polarized Prox1$^+$DCX$^+$ immature neuron with axon and dendrite. Over the next month, newborn cells mature into Prox1$^+$NeuN$^+$ neurons with spiny dendrites and long axons that project to CA3. See also Table S1. (*B*) Summary of the tangential distance of each neural progeny from its parental RGL at each developmental stage. IN, immature neuron; N, mature granule neuron; NB, neuroblast. Values represent mean ± SEM ($^*P < 0.01$; $^{\#}P \sim 1$; Wilcoxon rank-sum test with Bonferroni correction for multiple comparisons; test statistic, $z = -5.58$ and -0.72, respectively). (*C*) Histogram and cumulative distribution plot of the maximum distance between clonally related neural progeny for all clones, including non–RGL-containing clones. See Fig. S1 for a 2D SGZ plane projection of representative clones ($^*P < 0.1$; two-sample Kolmogorov–Smirnov test statistic: 0.38).

We next quantitatively determined the extent of tangential distribution of neuronal progeny in each clone under 2D SGZ projection. As opposed to measuring the distance of each newborn progeny to its mother RGL as in Fig. 1, we instead measured the maximum distance among all newborn progeny within each clone. The mean values were 43 ± 16 μm and 69 ± 19 μm, whereas the maximum values were 149 μm and 210 μm at 7 dpi and 1–2 mpi, respectively. The distribution of maximum distances was modestly shifted from 7 dpi to 1–2 mpi (Fig. 2*C*). The considerable spacing among neural progeny supports our model of neuronal migration as opposed to primarily motility of RGLs.

Vascular Substrate for Putative Tangential Migration. We then investigated a potential cellular mechanism underlying tangential migration of neuronal precursors in the adult hippocampus in vivo. Tangential migration of GABAergic interneurons has been shown to be facilitated by a combination of homotypic and heterotypic cellular interactions, such as migration in chains and along existing axonal processes, respectively (15). We therefore searched for potential substrates that could support tangential migration during adult hippocampal neurogenesis. In the adult dentate gyrus, BrdU-incorporating cells are known to be in close association with the vasculature (11). Indeed, we found that labeled neuroblasts mostly stayed in very close contact with CD31$^+$ vasculature (Fig. 3 *A* and *B* and Movie S2). Notably, these neuroblasts exhibited polarized organelles, such as GM130$^+$ Golgi apparatus (Fig. 3*C*) and γ-tubulin$^+$ centrosomes (Fig. 3*D*), characteristic of migrating, mobile cells (15).

Quantitative analysis further showed that, among all labeled cells, Tbr2$^+$DCX$^+$ and Tbr2$^-$DCX$^+$ neuroblasts were two major cell types in contact with the vasculature, either via cell soma or processes (Fig. 4*A*, *Left*). Eighty-eight percent of Tbr2$^+$DCX$^+$ and 80% of Tbr2$^-$DCX$^+$ cells with tangential processes were closely associated with the vasculature (Fig. 4*A*, *Right*). In contrast, Tbr2$^+$DCX$^-$ IPCs or Tbr2$^-$DCX$^+$ immature neurons with radial processes mostly lacked vascular contact (Fig. 4*A*). We further examined the interaction between neural progeny and endothelial cells at the ultrastructural level using electron microscopy. Remarkably, processes and soma of some labeled neuroblasts were in direct contact with blood vessels (Fig. 4*B*). These data support the model that neuroblasts represent the dominant cell stage of active migration via a vascular substrate.

Global View of Neural Precursors and Vascular Niche. To determine whether the general population of neural precursors exhibited properties similar to those clonally labeled in *Ascl1^{CreERT2}* mice, we developed a partial "whole-mount" preparation by sectioning the hippocampus parallel to the SGZ (Fig. 5*A* and Movie S3). This preparation enabled large sheets of the SGZ to be visualized in a single section. We first visualized CD31$^+$ vasculature and found a dense bed of blood vessels within the SGZ, in contrast to a sparse, columnar architecture of vessels within the granule cell layer (Fig. 5*B*). The SGZ vascular architecture may therefore be uniquely suited to supporting tangential migration of newborn progeny within the adult SGZ.

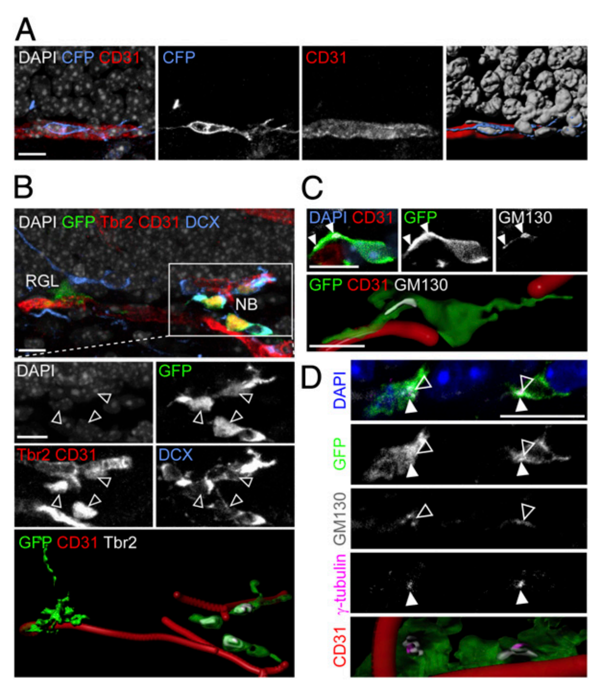

Fig. 3. Close association between tangentially migrating neuroblasts and blood vessels in the adult dentate gyrus. (*A*) Sample confocal images (*Left*) and 3D rendering (*Far Right*) of a CFP$^+$ clone at 7 dpi with a neuroblast whose soma and tangential process closely associated with a CD31$^+$ blood vessel. (*B*) Sample confocal image and 3D rendering of a GFP$^+$ clone at 7 dpi containing a parental RGL and dispersed Tbr2$^+$DCX$^+$ neuroblasts (open arrowheads) in close association with CD31$^+$ blood vessels (Movie S2). Note that CD31 and Tbr2 shared the same channel due to limited availability of channels but could be distinguished by different morphology (Tbr2, nuclear staining; CD31, tubular staining). (*C*) Sample confocal image and 3D rendering of a GFP$^+$ clone at 7 dpi with a neuroblast whose tangential process extended along a blood vessel and contained polarized GM130$^+$ Golgi apparatus (closed arrowheads) at its base, proximal to the cell soma. (*D*) Sample confocal image and 3D rendering of GFP$^+$ neuroblasts at 7 dpi with polarized γ-tubulin$^+$ centrosomes (closed arrowheads) and GM130$^+$ Golgi apparatus (open arrowheads) and in close association with CD31$^+$ blood vessels. (Scale bars, 10 μm.)

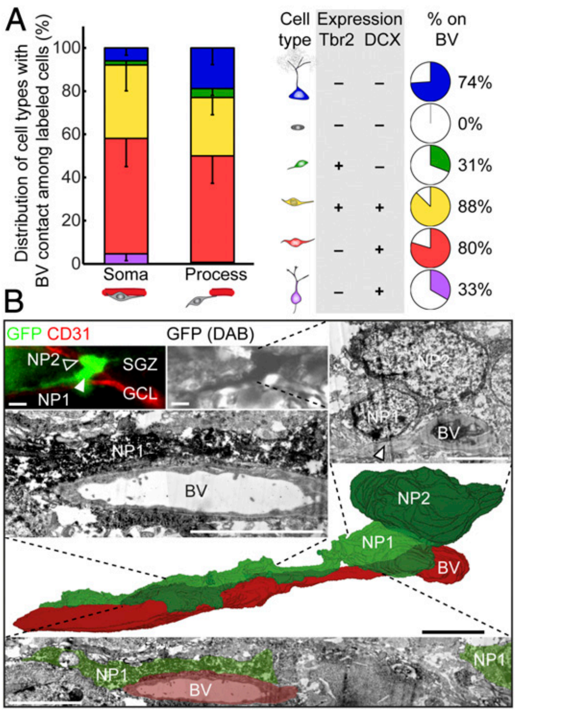

Fig. 4. Direct contact between tangentially migrating neuroblasts and blood vessels in the adult dentate gyrus. (*A*) (*Left*) Quantification of the distribution of various labeled precursors in close association with the vasculature at 7 dpi. Values represent mean ± SEM. (*Right*) Summaries of precursor cell molecular marker expression and the percentage of a given cell subtype in close association with the vasculature. BV, blood vessel. (*B*) Three-dimensional reconstruction, from serial electron microscopic sections, of a GFP^+ SGZ neuronal precursor (NP1; closed arrowhead) extending a tangential process along a blood vessel. The immunofluorescence-identified, immunoperoxidase-labeled cell (*Top*) sits alongside another neuronal precursor (NP2; open arrowhead) and apposes the blood vessel with both its tangential process (*Middle Left*) and its cell body (*Top Right*; arrowhead). (Scale bars, 5 μm.)

Using *Nestin-GFP* reporter mice (16) in combination with the same immunohistological and morphological markers used for clonal analysis (Fig. 2*A* and Table S1), we examined the association of SGZ progenitors with vasculature (Fig. 5*C*). Given that a fraction of different cell types would be in close proximity to blood vessels by chance, we simulated vascular association of the same number of each cell type randomly placed in the same SGZ space. We found that $Tbr2^+DCX^+$ or $Tbr2^-DCX^+$ neuroblasts were associated with $CD31^+$ blood vessels significantly above chance levels (Fig. 5*D* and Movie S4). These neuroblasts on blood vessels also contained polarized $GM130^+$ Golgi apparatus, characteristic of migrating cells (Fig. 5*E*). Together with findings from clonal analyses (Figs. 3 and 4), these results support a model whereby vasculature serves as a substrate for tangential migration of newborn neural progeny during adult hippocampal neurogenesis.

Discussion

In contrast to the prevailing model that glutamatergic neurons migrate radially whereas interneurons migrate tangentially during development, we demonstrated to our knowledge for the first time in the adult mammalian brain that neuroblast precursors of principal glutamatergic neurons exhibit significant tangential distribution away from their parental stem cells under physiological conditions. We revealed a two-step migration process during adult hippocampal neurogenesis in which significant tangential migration of neuroblasts is followed by limited radial migration of immature neurons (Fig. 6). Tangentially migrating neuroblasts may use the vasculature as a migration substrate, revealing an important role of this neurogenic niche component (Fig. 6).

Our finding of dominant tangential migration of neural precursors of principal glutamatergic dentate granule cells in the adult brain is a departure from the classic radial unit hypothesis of embryonic cortical development (1). Although early studies described tangential migration of presumed excitatory neurons in the embryonic cortex, they may have actually been describing tangentially migrating inhibitory neurons, which were discovered later (17). Interestingly, at least some rare (18), although usually transient (19, 20), populations of excitatory cortical neurons migrate tangentially in the developing brain. Tangential migration of neural precursors in the developing hippocampus has previously only been observed in early postnatal developmental stages, during which the hippocampus is still immature and marked by ongoing growth and development (21, 22). It may be that radial and tangential migration modes are not specific to neurons releasing a specific neurotransmitter. Indeed, in the cerebellum, inhibitory principal Purkinje neurons exhibit radial migration, whereas excitatory modulatory granule neurons migrate tangentially as well as radially (23). A very small number of glutamatergic modulatory interneurons are also generated in the adult SVZ and migrate tangentially to the olfactory bulb (24). Motor neurons in the spinal cord possess both radial and tangential migration (25). Additionally, neurons originating from the diencephalon can migrate tangentially to populate the amygdala, a telencephalic nucleus (26).

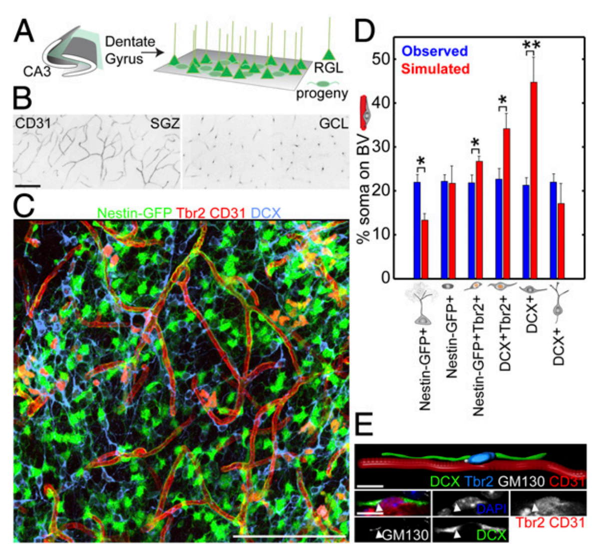

Fig. 5. Neuroblast–vasculature interaction using a partial whole-mount dentate gyrus SGZ preparation. (*A*) Schematic illustration of the partial whole-mount SGZ preparation (Movie S3). (*B*) $CD31^+$ blood vessels using a whole-mount preparation visualized in SGZ (*Left*) and GCL (*Right*). (Scale bar, 100 μm.) (*C*) Sample projected confocal image of *Nestin-GFP* tissue from a partial whole-mount preparation immunostained for Tbr2, CD31, and DCX (Movie S4). (Scale bar, 100 μm.) (*D*) Quantification of the vascular association of different cell types expressing combinations of Nestin-GFP, Tbr2, and DCX using a partial whole-mount preparation to view the population of progenitors in the SGZ. Association was defined as having cell soma on a blood vessel and compared with simulated random distributions of the same numbers of cells in the same space. Values represent means ± SEM [$n = 3$ animals; $^*P < 0.05$; $^{**}P < 0.01$; one-tailed unpaired Student's t test, observed > simulated; $Tbr2^+$: $t(4) = 2.20$; $Tbr2^+DCX^+$: $t(4) = 2.44$; DCX^+ (neuroblast): $t(4) = 3.76$]. (*E*) Sample confocal image and 3D rendering of a $Tbr2^+DCX^+$ neuroblast migrating on a $CD31^+$ blood vessel with polarized $GM130^+$ Golgi apparatus (closed arrowhead) from a partial whole-mount preparation in a *Nestin-GFP* mouse. (Scale bars, 10 μm.)

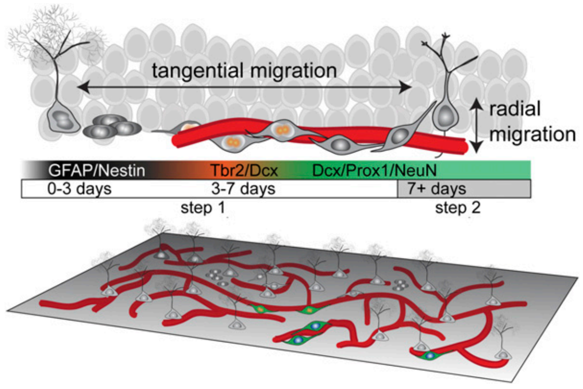

Fig. 6. Two-step model for neuronal migration during adult hippocampal neurogenesis. During adult hippocampal neurogenesis, radial glia-like cells give rise to Tbr2$^+$ intermediate progenitor cells within 3 d. In the next 4 d, the cells become DCX$^+$ proliferating neuroblasts that extend long processes tangential to the SGZ and contact blood vessels directly. During this phase, neuroblasts use blood vessels as a substrate to migrate tangentially away from their parental RGL. After 7 d, newborn neural progeny extend radial dendritic processes and develop into NeuN$^+$Prox1$^+$ dentate granule neurons and exhibit limited radial migration through the granule cell layer. (*Lower*) Global-view illustration of RGLs, neural progeny, and vasculature in the adult SGZ.

Here we have described an example of tangential migration of neuronal precursors of excitatory principal neurons in the adult mammalian brain. The magnitude of migration observed, although significant and not due to cell displacement upon division, is much less than that of migrating SVZ neuroblasts or even radially migrating neocortical neurons. This may be due to differences in tissue architecture. Neuroblasts in the SVZ are born far from their target brain region and the neocortex is a multilayered structure, both requiring cells to travel longer distances to populate all target regions. By comparison, the dentate gyrus is a thin single-layer sheet whereby newborn neurons were presumed, before the present study, to be born, develop, and integrate all in the same location. Due to the limitation of single-color reporters in resolving different clones and the probabilities of clonality calculated from our simulations, we took an inherently conservative approach by imposing a 300-μm maximum for clone diameter. Our reported magnitude of tangential migration distance may therefore be an underestimation.

The vasculature has been proposed to be a crucial niche component for adult neurogenesis in both the SGZ and SVZ (8–11); however, its functional role is not well-understood. We showed that neuroblasts exhibit several features of migrating cells, such as polarized organelle distribution, and that they display a tight, direct association with the vasculature at cellular and ultrastructural levels. Although our data leave open the possibility of vasculature-independent tangential migration, our findings suggest that one function of the vascularized niche is to support migration of neuronal progeny away from their parental origin. Interestingly, GABAergic neurons generated in the adult SVZ have also been shown to migrate along blood vessels in the rostral migratory stream (27, 28) and toward injury sites following stroke (29). Thus, in the adult brain, the vasculature may serve as a common substrate for migration of different neuronal subtypes. This mechanism to support cell migration may also be important during early development, because vascular outgrowth often precedes neural outgrowth, and migrating cells can be found in regions lacking classic substrates such as glial fibers (30, 31).

We and others have previously only documented radial migration during adult hippocampal neurogenesis (32, 33), having been limited to population-level analyses that lacked lineage relationship information of individual stem cells and their progeny. Our current approach permits clonal analysis of activating adult dentate RGLs using the *Ascl1*^{CreERT2} knockin mouse line (13) and direct examination of cell dispersion of individual newborn progeny with respect to their parental RGL. With the high temporal and spatial resolution our approach allows, we were able to directly compare tangential and radial migration of individual cells for the first time, to our knowledge. Interestingly, the two forms of migration appeared to be temporally segregated, with tangential migration preceding and exceeding radial migration. Together, these data suggest that independent mechanisms may regulate the two modes of migration. Future studies combining our clonal analysis with conditional gene inactivation could elucidate shared or independent molecular mechanisms governing different forms of migration.

We also developed a partial whole-mount preparation to optimize visualization of the SGZ niche and showed that the general population of neuroblasts is in close contact with the blood vessel network and exhibits polarized Golgi apparatus, characteristic of migrating cells. This preparation will allow for systematic characterization of the complete global architecture of the hippocampal niche in the future. Such a characterization could potentially reveal important motifs for understanding the underlying structure of the vascular network and migrating cells that we have observed. Ultimately, our technique can help broaden our knowledge of general principles of neurogenic niches, especially in combination with knowledge gained from similar approaches in the adult SVZ (8–10).

Our clonal analyses of activating radial glia-like neural stem cells reveal a previously unrecognized mode of neuronal migration during adult hippocampal neurogenesis. Given that adult neural stem cells are dynamically regulated by their local environment, including neuronal activity modulation (34, 35), our findings have significant implications for understanding how individual neural stem cells could impact the function of the existing microcircuitry via delivery of newborn neurons that are primed to undergo a critical period of enhanced plasticity (36). Our findings also provide a framework in which to investigate the aberrant migration of newborn granule cells under pathological conditions, such as epilepsy (37, 38). In addition, the identification of a novel mode of glutamatergic cell migration tangentially along the vasculature suggests a strategy for overcoming current challenges in targeting glutamatergic neurons to injured or degenerating regions for successful cell-transplantation therapy in the adult mammalian brain (39). Together, our results suggest that diverse modes of migration may be ubiquitous among different neuronal classes in the adult mammalian brain, providing important conceptual groundwork for future studies of neural development, plasticity, regeneration, repair, and brain disorders.

Materials and Methods

Animals and Tamoxifen Administration. *Ascl1*^{CreERT2}*;Rosa-YFP*$^{f/+}$ and *Ascl1*^{CreERT2}*;Confetti*$^{f/+}$ mice and *Nestin-GFP* transgenic mice were used. All mice in the study were backcrossed to the C57BL/6 background for at least six generations. Animals were housed in a 14-h light/10-h dark cycle with free access to food and water. Tamoxifen (66.67 mg/mL; Sigma; T5648) was prepared in a 5:1 corn oil (Sigma)-to-ethanol mixture. To achieve sparse labeling for clonal analysis (~8–16 clones per hemisphere), a single dose of tamoxifen (77.5 mg/kg for the *Rosa-YFP*$^{f/+}$ reporter; 250 mg/kg for the *Confetti*$^{f/+}$ reporter) was intraperitoneally injected into adult 8- to 10-wk-old male and female mice. Animal procedures were performed in accordance with institutional guidelines of the Johns Hopkins University School of Medicine.

Tissue Processing, Immunostaining, and Confocal Imaging. Serial 40-μm-thick coronal sections were prepared for immunohistology as described (12). For partial whole-mount dentate gyrus SGZ preparations the whole hippocampus was dissected from the cortex and mounted dentate side-up on a frozen sliding microtome, and serial 50-μm horizontal sections were collected. All antibodies used are listed in *SI Materials and Methods*. Confocal images were taken to confirm cell identity according to immunohistological and morphological properties (Fig. 2*A* and Table S1).

Image Processing and Data Analysis. Clonal analysis and simulations to estimate the probability of two cells belonging to a clone from 3D reconstructed adult dentate gyri were performed as previously described (12). Clones that spanned multiple serial sections were reconstructed using Reconstruct software (John C. Fiala, NIH, Bethesda). Aligned images were exported at full resolution for 3D visualization into Imaris (Bitplane). Cells and vasculature were identified, localized, and digitized into 3D space in Imaris according to distinct morphological and molecular markers (Fig. 2*A* and Table S1). Data were exported to Matlab (The MathWorks) for analysis. Distance measurements at the clonal level were collected from 7 hemispheres (five animals) at 3 dpi, 9 hemispheres (six animals) at 7 dpi, and 12 hemispheres (seven animals) at 1–2 mpi. For vasculature association analysis at the clonal level, all labeled clones and percentages of vasculature association were quantified and averaged across 10 hemispheres (five animals). For vasculature association analysis at the population level, all cells in a horizontal section from three *Nestin-GFP* animals were quantified. Simulated vasculature associations (Fig. 5*D*) were performed by randomly placing cells in the same 2D SGZ space, as estimated by a third-degree polynomial plane fit. One hundred iterations of the simulation were performed for each cell type.

Electron Microscopy Analysis. Adult C57BL/6 female mice were stereotaxically injected with retrovirus expressing GFP (40) and processed 2 d after injection. Fifty-micrometer-thick coronal sections containing clearly labeled newborn progeny in close association with the $CD31^+$ vasculature were sequentially incubated in biotinylated anti-GFP, avidin–biotin–peroxidase complex, 3,3-diaminobenzidine (DAB) peroxidase, and 1% osmium tetroxide before being dehydrated and lifted into resin. Seventy-nanometer-thick serial sections were collected onto copper grids and contrasted with a lead stain, and serial images were taken using a Philips CM10 transmission electron microscope to create 3D reconstructions with Fiji ImageJ software (41).

Statistical Analysis. Statistical analysis methods can be found in *SI Materials and Methods*.

ACKNOWLEDGMENTS. We thank A. Saghatelyan and members of the H.S. and G.-l.M. laboratories for discussion, G. Enikolopov for *Nestin-GFP* mice, and Y. Cai and L. Liu for technical support. This work was supported by the NIH (NS048271 and MH105128; to G.-l.M.) and Dr. Miriam and Sheldon G. Adelson Medical Research Foundation (G.-l.M.), NIH (NS047344; to H.S.), Swiss National Science Foundation (PP00A-119026/1; to N.T.), Foundation Leenaards (J.M.), and a predoctoral fellowship from the Children's Tumor Foundation (to G.J.S.).

1. Rakic P (2009) Evolution of the neocortex: A perspective from developmental biology. *Nat Rev Neurosci* 10(10):724–735.
2. Corbin JG, Nery S, Fishell G (2001) Telencephalic cells take a tangent: Non-radial migration in the mammalian forebrain. *Nat Neurosci* 4(Suppl):1177–1182.
3. Fuentealba LC, Obernier K, Alvarez-Buylla A (2012) Adult neural stem cells bridge their niche. *Cell Stem Cell* 10(6):698–708.
4. Ming Gl, Song H (2011) Adult neurogenesis in the mammalian brain: Significant answers and significant questions. *Neuron* 70(4):687–702.
5. Lois C, Alvarez-Buylla A (1994) Long-distance neuronal migration in the adult mammalian brain. *Science* 264(5162):1145–1148.
6. Braun SMG, Jessberger S (2013) Adult neurogenesis in the mammalian brain. *Front Biol* 8(3):295–304.
7. Toni N, et al. (2007) Synapse formation on neurons born in the adult hippocampus. *Nat Neurosci* 10(6):727–734.
8. Mirzadeh Z, Merkle FT, Soriano-Navarro M, Garcia-Verdugo JM, Alvarez-Buylla A (2008) Neural stem cells confer unique pinwheel architecture to the ventricular surface in neurogenic regions of the adult brain. *Cell Stem Cell* 3(3):265–278.
9. Shen Q, et al. (2008) Adult SVZ stem cells lie in a vascular niche: A quantitative analysis of niche cell-cell interactions. *Cell Stem Cell* 3(3):289–300.
10. Tavazoie M, et al. (2008) A specialized vascular niche for adult neural stem cells. *Cell Stem Cell* 3(3):279–288.
11. Palmer TD, Willhoite AR, Gage FH (2000) Vascular niche for adult hippocampal neurogenesis. *J Comp Neurol* 425(4):479–494.
12. Bonaguidi MA, et al. (2011) In vivo clonal analysis reveals self-renewing and multipotent adult neural stem cell characteristics. *Cell* 145(7):1142–1155.
13. Kim EJ, Ables JL, Dickel LK, Eisch AJ, Johnson JE (2011) Ascl1 (Mash1) defines cells with long-term neurogenic potential in subgranular and subventricular zones in adult mouse brain. *PLoS One* 6(3):e18472.
14. Berg DA, et al. (2015) Tbr2-expressing intermediate progenitor cells in the adult mouse hippocampus are unipotent neuronal precursors with limited amplification capacity under homeostasis. *Front Biol* 10(3):262–271.
15. Ghashghaei HT, Lai C, Anton ES (2007) Neuronal migration in the adult brain: Are we there yet? *Nat Rev Neurosci* 8(2):141–151.
16. Encinas JM, Vaahtokari A, Enikolopov G (2006) Fluoxetine targets early progenitor cells in the adult brain. *Proc Natl Acad Sci USA* 103(21):8233–8238.
17. Marín O, Rubenstein JL (2001) A long, remarkable journey: Tangential migration in the telencephalon. *Nat Rev Neurosci* 2(11):780–790.
18. Britanova O, et al. (2006) A novel mode of tangential migration of cortical projection neurons. *Dev Biol* 298(1):299–311.
19. Bielle F, et al. (2005) Multiple origins of Cajal-Retzius cells at the borders of the developing pallium. *Nat Neurosci* 8(8):1002–1012.
20. Teissier A, et al. (2010) A novel transient glutamatergic population migrating from the pallial-subpallial boundary contributes to neocortical development. *J Neurosci* 30(31):10563–10574.
21. Seki T, Namba T, Mochizuki H, Onodera M (2007) Clustering, migration, and neurite formation of neural precursor cells in the adult rat hippocampus. *J Comp Neurol* 502(2):275–290.
22. Li G, Pleasure SJ (2014) The development of hippocampal cellular assemblies. *Wiley Interdiscip Rev Dev Biol* 3(2):165–177.
23. Komuro H, Yacubova E, Yacubova E, Rakic P (2001) Mode and tempo of tangential cell migration in the cerebellar external granular layer. *J Neurosci* 21(2):527–540.
24. Brill MS, et al. (2009) Adult generation of glutamatergic olfactory bulb interneurons. *Nat Neurosci* 12(12):1524–1533.
25. Leber SM, Sanes JR (1995) Migratory paths of neurons and glia in the embryonic chick spinal cord. *J Neurosci* 15(2):1236–1248.
26. García-Moreno F, et al. (2010) A neuronal migratory pathway crossing from diencephalon to telencephalon populates amygdala nuclei. *Nat Neurosci* 13(6):680–689.
27. Snapyan M, et al. (2009) Vasculature guides migrating neuronal precursors in the adult mammalian forebrain via brain-derived neurotrophic factor signaling. *J Neurosci* 29(13):4172–4188.
28. Whitman MC, Fan W, Rela L, Rodriguez-Gil DJ, Greer CA (2009) Blood vessels form a migratory scaffold in the rostral migratory stream. *J Comp Neurol* 516(2):94–104.
29. Grade S, et al. (2013) Brain-derived neurotrophic factor promotes vasculature-associated migration of neuronal precursors toward the ischemic striatum. *PLoS One* 8(1): e55039.
30. Saghatelyan A (2009) Role of blood vessels in the neuronal migration. *Semin Cell Dev Biol* 20(6):744–750.
31. Tam SJ, Watts RJ (2010) Connecting vascular and nervous system development: Angiogenesis and the blood-brain barrier. *Annu Rev Neurosci* 33:379–408.
32. Altman J, Das GD (1966) Autoradiographic and histological studies of postnatal neurogenesis. I. A longitudinal investigation of the kinetics, migration and transformation of cells incorporating tritiated thymidine in neonate rats, with special reference to postnatal neurogenesis in some brain regions. *J Comp Neurol* 126(3): 337–389.
33. Duan X, et al. (2007) Disrupted-In-Schizophrenia 1 regulates integration of newly generated neurons in the adult brain. *Cell* 130(6):1146–1158.
34. Song J, et al. (2012) Neuronal circuitry mechanism regulating adult quiescent neural stem-cell fate decision. *Nature* 489(7414):150–154.
35. Jang MH, et al. (2013) Secreted frizzled-related protein 3 regulates activity-dependent adult hippocampal neurogenesis. *Cell Stem Cell* 12(2):215–223.
36. Ge S, Yang CH, Hsu KS, Ming Gl, Song H (2007) A critical period for enhanced synaptic plasticity in newly generated neurons of the adult brain. *Neuron* 54(4):559–566.
37. Parent JM, et al. (1997) Dentate granule cell neurogenesis is increased by seizures and contributes to aberrant network reorganization in the adult rat hippocampus. *J Neurosci* 17(10):3727–3738.
38. Jessberger S, et al. (2007) Seizure-associated, aberrant neurogenesis in adult rats characterized with retrovirus-mediated cell labeling. *J Neurosci* 27(35):9400–9407.
39. Ladewig J, Koch P, Brüstle O (2014) Auto-attraction of neural precursors and their neuronal progeny impairs neuronal migration. *Nat Neurosci* 17(1):24–26.
40. Song J, et al. (2013) Parvalbumin interneurons mediate neuronal circuitry-neurogenesis coupling in the adult hippocampus. *Nat Neurosci* 16(12):1728–1730.
41. Schindelin J, et al. (2012) Fiji: An open-source platform for biological-image analysis. *Nat Methods* 9(7):676–682.